



Research Article

Evaluating Simplified Crop Water Stress Index Derived from UAV Thermal Imagery for Water Status Assessment in Wheat Crop under Diverse Irrigation and Nitrogen Application

SUPRIYO DHARA¹, RAJEEV RANJAN^{1*}, RABI N. SAHOO¹, MONALISHA PRAMANIK², JOYDEEP MUKHERJEE¹, MAHESH KUMAR³, PRAVIN KUMAR UPADHYAY⁴ AND SANDEEP KUMAR⁵

¹Division of Agricultural Physics, ICAR-Indian Agricultural Research Institute, New Delhi-110012

²Water Technology Centre, ICAR-Indian Agricultural Research Institute, New Delhi-110012

³Division of Plant Physiology, ICAR-Indian Agricultural Research Institute, New Delhi-110012

⁴Division of Agronomy, ICAR-Indian Agricultural Research Institute, New Delhi-110012

⁵Division of Environment Science, ICAR-Indian Agricultural Research Institute, New Delhi-110012

ABSTRACT

Effective water management is essential to enhance productivity of wheat and to improve input use efficiency, particularly in the present resource-limited scenario. Unmanned aerial vehicle (UAV)-based remote sensing has emerged as an advanced technology for real-time monitoring of crop water status. To understand the applicability of Simplified Crop Water Stress Index ($CWSI_{si}$), an index derived from UAV thermal imagery for assessing water status of wheat crop under variable irrigation and nitrogen application, a field experiment was conducted on wheat (cv HD2967) in a Split plot design having three irrigation levels (I1 to I3) as main plot and six nitrogen levels (N1 to N6) as sub plots. UAV thermal and multispectral imageries were collected concurrently with biophysical measurements of relative leaf water content (RWC), stomatal conductance (Gs), and transpiration rate (Tr) during reproductive stage. Background soil pixels were removed from thermal images using NDVI co-registration method and $CWSI_{si}$ were calculated from the derived canopy temperature information. Analysis was performed to study the variation of water status as well as the correlation among the index and biophysical observations. Canopy temperature derived through NDVI co-registration method showed robust correlation with ground-truth data ($R^2 = 0.92$). The $CWSI_{si}$, derived from canopy temperature distribution in thermal imagery, showed good linear relationships with RWC ($R^2 = 0.73$), Gs ($R^2 = 0.63$), and Tr ($R^2 = 0.73$) during the reproductive stage. Significant negative correlations were observed between $CWSI_{si}$ and RWC ($r = -0.855$), Gs ($r = -0.793$), Tr ($r = -0.857$). Simplified crop water stress index approach using UAV thermal imaging may help in rapid, real-time monitoring of water status of crops, assisting efficient water and nutrient management to obtain optimum input use efficiency and yield. However, this method needs further works under different crops and conditions before large scale application.

Key words: Crop water stress index, Irrigation and nitrogen, Thermal imagery, UAV, Wheat

Introduction

Wheat (*Triticum aestivum* L.) is one of the most important cereal crops, contributing significantly to

global food and nutritional security. India is the world's second-largest wheat-producing country where it is primarily grown during the *Rabi* season. Irrigation is applied throughout the wheat growing period to meet the crop water requirement. Irrigation

*Corresponding author, Email: rajeev4571@gmail.com

is available for over 94% of the wheat fields in India (MAFW, 2017). Due to limited water resources, anomalous precipitation, climate change and increased demand for water from other sectors, it is essential to manage available water resources efficiently for crop production in irrigated areas. Besides irrigation, nitrogen is another key input for wheat crop growth and productivity. Crop nitrogen and water status are often related to availability of each other which is known as co-limitation. It determines the biomass output (Sadras, 2004). Efficient water management requires timely crop water status monitoring. It helps to reduce the loss of both water and applied nitrogen increasing their use efficiency. It also avoids irreversible losses due to prolonged water stress by timely detection.

Recent advances in unmanned aerial vehicle (UAV) technology along with suitable sensors enable rapid, real-time, non-destructive ways to monitor crop biotic and abiotic stress with more detailed data with higher spatial and temporal resolution than the conventional soil moisture measurement, meteorological methods, physiological measurements, or other ground-based and space-borne remote sensing approaches (Gago *et al.*, 2015). A portable thermal camera on board a UAV can capture the whole field's temperature information. Canopy temperature information can be obtained from it after removing the soil background pixels through proper image processing techniques (Zhou *et al.*, 2021). Crop water stress index (CWSI), a canopy temperature-based index proposed by Idso *et al.* (1981), has been utilized for decades in different forms for quantifying plant water status or water stress. CWSI has various forms depending upon the approaches of calculating the minimum and maximum value of canopy-air temperature difference which are affected by various environmental factors such as vapour pressure deficit (VPD), net radiation, and wind speed (Jackson *et al.*, 1977; Idso *et al.*, 1977). Empirical, theoretical or artificial reference surface approaches of CWSI calculation have several limitations being data-intensive, complex to calculate and dependent on several other meteorological parameters. Bian *et al.* (2019) proposed a Simplified crop water stress index (CWSI_{si}) to evaluate cotton water stress, which only requires parameters from the canopy temperature histogram. It showed a better

correlation with stomatal conductance and transpiration rate than the empirical CWSI, statistical CWSI and selected spectral indices. Although CWSI_{si} showed good performance in water stress monitoring of cotton crops over other CWSI approaches and spectral indices, still it is not evaluated enough in major cereal crops having a different canopy structure. Different nitrogen application scenarios were also not considered in those studies. This study aims to evaluate the applicability of CWSI_{si} to assess the crop water status of wheat under varying irrigation and nitrogen application by studying the correlation among CWSI_{si} and biophysical observations of water status e.g. relative leaf water content (RWC), stomatal conductance (Gs) and transpiration rate (Tr).

Material and Methods

Field Experimentation

The experiment was conducted at the experimental farm (Main Block 12B) of ICAR-Indian Agricultural Research Institute, New Delhi, India on wheat crop (cv HD2967) during *Rabi* season of 2023-24. The climate of the site is sub-tropical semi-arid with hot, dry summer and severe, short winter. A cumulative of 54.6 mm rainfall was received during the growing period of wheat in that season. The soil of the experimental plots was sandy loam (Typic Haplustept) of the Gangetic alluvial origin, neutral to slightly alkaline (pH 7.96), had high organic carbon (0.76%), phosphorus (51.7 kg ha⁻¹) and potassium (394 kg ha⁻¹) but low nitrogen content (197.4 kg ha⁻¹). The experiment was conducted in a split plot design with three replications. It had three irrigation levels (number of irrigations based on critical growth stages) in main plots i.e. I1: no irrigation; I2: irrigations at crown root initiation (CRI, 21 days after sowing (DAS)) and ear emergence (90 DAS); I3: irrigations at CRI (21 DAS), late tillering (44 DAS), late jointing (66 DAS), ear emergence (90 DAS) and milking-soft dough stage (120 DAS). In each irrigation, 50 mm water was applied as basin irrigation by measuring through a Starflow doppler flowmeter (Unidata Pty. Ltd., Australia) attached in irrigation channel. There were six nitrogen levels in the sub plots, i.e., N1: no nitrogen (control), N2: 40

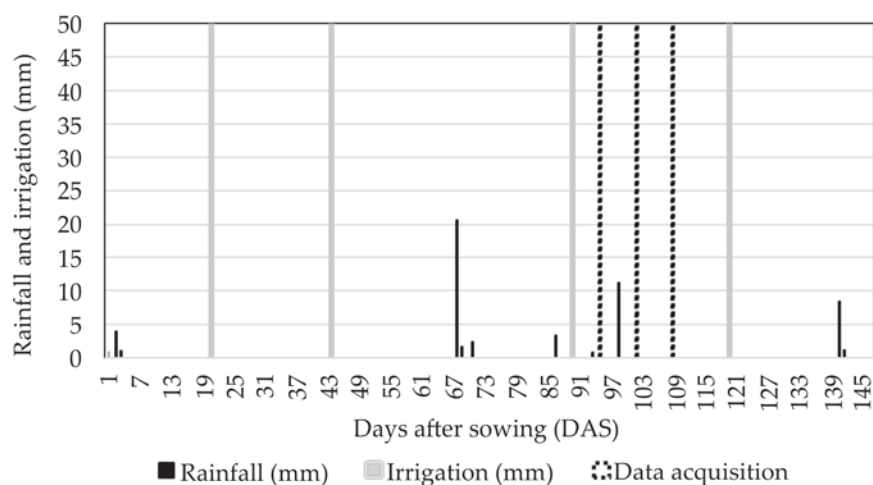


Fig. 1. Dates and amounts of rainfall, irrigations and dates of data acquisition during wheat growing period

kg N ha⁻¹ (as basal), N3: 80 kg N ha⁻¹ (two equal splits), N4: 120 kg N ha⁻¹, N5: 160 kg N ha⁻¹ and N6: 200 kg N ha⁻¹ (three equal splits). Each subplot area was of 84 m² (4.2 m × 20 m). Nitrogen was applied as prilled urea through manual broadcasting according to treatment wise split doses at the time of sowing (basal), 25 DAS and 50 DAS. Phosphorus and potassium were applied as basal in all plots as single super phosphate @ 60 kg P₂O₅ ha⁻¹ and muriate of potash @ 60 kg K₂O ha⁻¹, respectively. The crop was sown on 25th November, 2023 at 4-5 cm soil depth maintaining a row spacing of 22.5 cm by a tractor-drawn seed drill at a seed rate of 100 kg ha⁻¹. It was harvested on 20th April, 2024. Important dates and quantities regarding irrigation, rainfall and data acquisitions are presented in Fig. 1.

UAV image acquisition

Thermal and multispectral images were collected from an imaging hexacopter UAV (General Aeronautics Pvt Ltd, Bengaluru, India) using an uncooled radiometric thermal camera (model: Vue Pro R, Teledyne FLIR LLC, USA) and five-band multispectral camera (model: RedEdge MX, Micasense, Inc., USA), respectively. The imaging was done from a height of 30 m, maintaining the flight speed at 5 m s⁻¹, frontal and side overlap at 70% under clear sky and fair-weather conditions. Radiometric calibration of multispectral imagery was done using a calibrated reflectance panel (Micasense, Inc., USA) before and after each flight. The UAV, ground control device, and sensors used are illustrated in Fig. 2, with the sensors' specifications

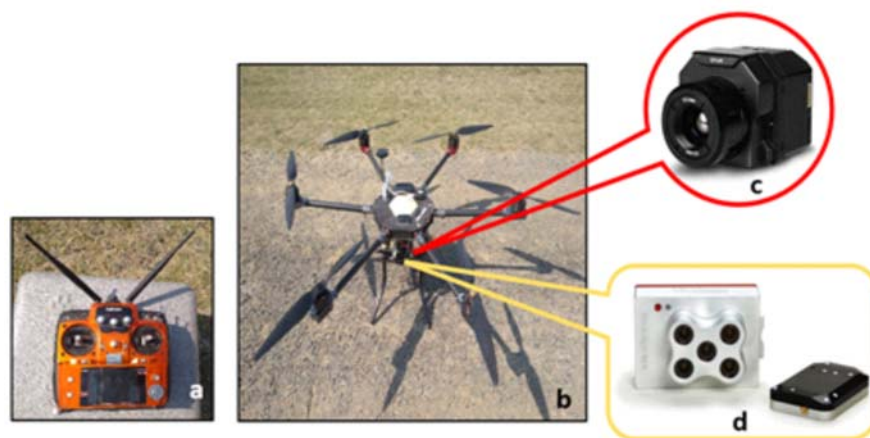


Fig. 2. The imaging system consisting (a) UAV transmitter, (b) hexacopter UAV, (c) thermal camera and (d) multispectral camera with Downwelling Light Sensor (DLS)

Table 1. Specifications of the thermal and multispectral sensors used for image acquisition

Multispectral camera (Micasense RedEdge MX)		Thermal camera (FLIR Vue Pro R)	
Resolution	1280 × 960	Resolution	640 × 512
Focal length	5.4 mm	Focal length	13 mm
Field of view	47.2° H × 35.4° V	Field of view	45° H × 37° V
Output	12 bits	GSD at 30 m	4 cm/pixel
Ground sampling distance (GSD) at 30 m	2 cm/pixel	Spectral band	7.5 - 13.5 µm
Spectral bands(central wavelength, bandwidth)	Blue (475nm, 20nm), Green (560nm, 20nm), Red (668nm, 10nm), NIR (840nm, 40nm) and Red Edge (717nm, 10nm)	Accuracy	± 5%

listed in Table 1. Image data were collected on three different dates at the reproductive stage: 95 DAS, 102 DAS, and 109 DAS, between 12:00 PM and 2:00 PM. A malfunction of the thermal camera caused some missing plots in the imagery of 109 DAS. However, at least one plot from each treatment combination was captured and used for further analysis.

Image processing and simplified crop water stress index (CWSI_{st}) calculation

The methodology of image processing and the index calculation is presented in Fig. 3. The individual thermal and multispectral images were mosaiced using Pix4Dmapper software (Pix4D, Switzerland) and Normalized Difference Vegetation Index (NDVI) maps were generated. Subsequent processing steps were conducted in ArcMap 10.3 software (ESRI, Inc., USA). The NDVI images were utilized to isolate pure canopy pixels from soil pixels present in the thermal imagery through a co-registration approach. NDVI images (initial pixel size 2 cm) were resampled to 4 cm pixel size using the nearest neighbour method to match the thermal imagery's pixel size and image-to-image registration was performed using first-order polynomial (affine) transformation. To separate vegetation and non-vegetation pixels, a binary raster was generated from the NDVI image using ISODATA unsupervised classification. The binary raster was overlaid on co-registered thermal image to extract only the vegetation pixels. Non-target vegetations in irrigation channels and bunds were removed using manually created polygons of the experimental plots. This

process resulted in the retrieval of thermal imagery containing pixels representing wheat crop canopy only. Average canopy temperatures for each plot were calculated. The temperature distribution tables and histograms for the thermal images were generated in MS Excel (Microsoft Corporation, WA, USA) using the unique temperature values and corresponding pixel counts or frequency. The simplified crop water stress index (CWSI_{si}) was calculated and mapped using the Eq. (1) (Bian *et al.*, 2019):

$$CWSI_{si} = (T_{canopy} - T_{wet}) / (T_{dry} - T_{wet}) \quad \dots \text{Eq. (1)}$$

where, T_{canopy} is pixelwise canopy temperature, T_{wet} is the average of the lowest 5% and T_{dry} is the average of the highest 5% of the canopy temperature histogram (Liu *et al.*, 2024). The T_{wet} and T_{dry} values for each day were calculated from the canopy temperature distribution table and were normalized between 0 to 1 using minimum-maximum normalization where 0 and 1 indicates non-stressed and maximum stress, respectively.

Ground truth canopy temperature and biophysical observations

Ground truth canopy temperature, relative leaf water content (RWC), transpiration rate (Tr) and stomatal conductance (Gs) were measured or sampled (for RWC) on the same days concurrently with image acquisition. Ground truth canopy temperature was measured using a handheld infrared thermometer (model: AGRI-THERM III - 6110L, Everest Interscience, Inc., USA) to evaluate the canopy temperature extracted from thermal imagery

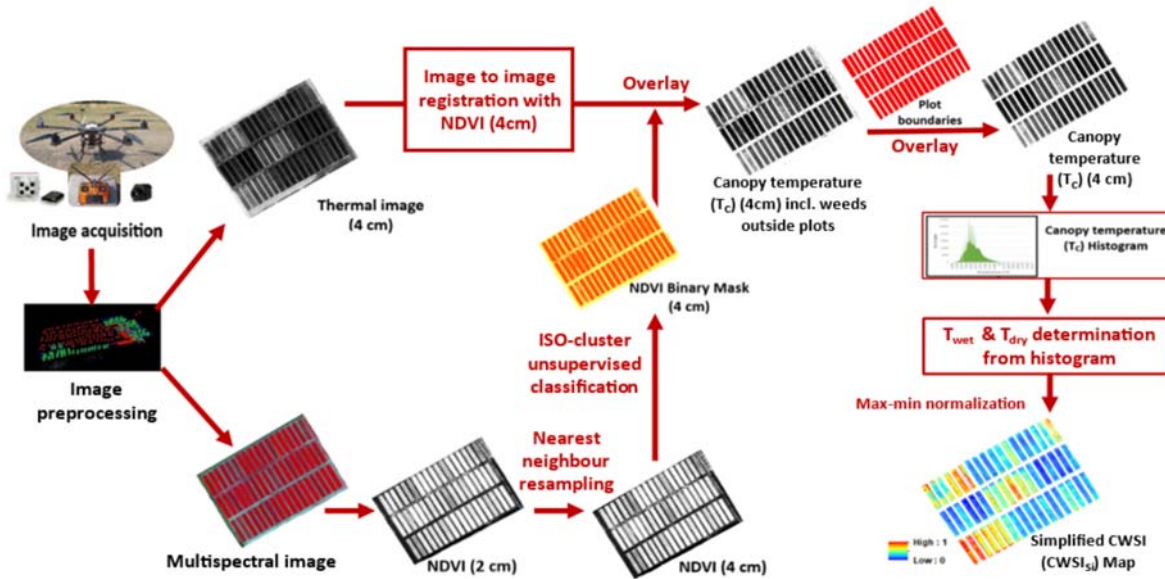


Fig. 3. Steps of image processing and simplified crop water stress index ($CWSI_{si}$) calculation

through the NDVI co-registration method. The instrument operates at a spectral range of 8 to 14 μm and has the accuracy of $\pm 0.25^\circ\text{C}$ for 0 to 50°C measurement range. Emissivity was set to 0.98 for the canopy temperature measurement of wheat crop (Bashir *et al.*, 2008). Canopy temperature was measured from a height of 1.5 m above the ground (Nielsen and Halvorson, 1991) at 45° angle with the horizon (Balota *et al.*, 2007) immediately following UAV image acquisition.

Relative leaf water content (RWC) was determined following the standing rehydration method (Arndt *et al.*, 2015) using disease-free flag leaf samples collected from each plot just before UAV flight. RWC values were calculated using the Eq (2).

$$RWC (\%) = \frac{(\text{leaf fresh weight} - \text{leaf dry weight})}{(\text{leaf turgid weight} - \text{leaf dry weight})} \times 100$$

.... Eq. (2)

Stomatal conductance (G_s) and transpiration rate (Tr) were measured using LI-6400 portable photosynthesis system (LiCOR Biosciences, Lincoln, NE, USA) (Evans and Santiago, 2014) between 11.30 am and 12.30 pm from clean, healthy flag leaves within each plot.

Statistical analysis

Analysis of variance (ANOVA) for split-plot was

performed for the values of different parameters using SPSS Statistics software (version 26.0, IBM Corporation, USA) to assess the significance of treatment effects. The $CWSI_{si}$ values of missing plots at 109 DAS were replaced by means imputation. To compare the means of main factors and perform all pairwise comparisons, Duncan's Multiple Range Test (DMRT) was applied at 5% significance level. The coefficient of determinations (R^2) was calculated to examine the linear relationship of $CWSI_{si}$ with biophysical parameters of water status. Additionally, Pearson's correlation coefficient (r) was computed to assess linear correlations among the various parameters. The workflow of the study is presented in Fig. 4.

Results and Discussion

Evaluation of canopy temperature extracted from UAV thermal imagery

A strong linear relationship was observed between the canopy temperature extracted from the UAV thermal imagery and the corresponding ground truth data, with an R^2 of 0.92 for treatment wise average values across the three dates, as presented in Fig. 5. Notably, the ground truth canopy temperatures were found to be generally higher than those extracted from the UAV thermal imagery, which may be attributed to more incoming soil

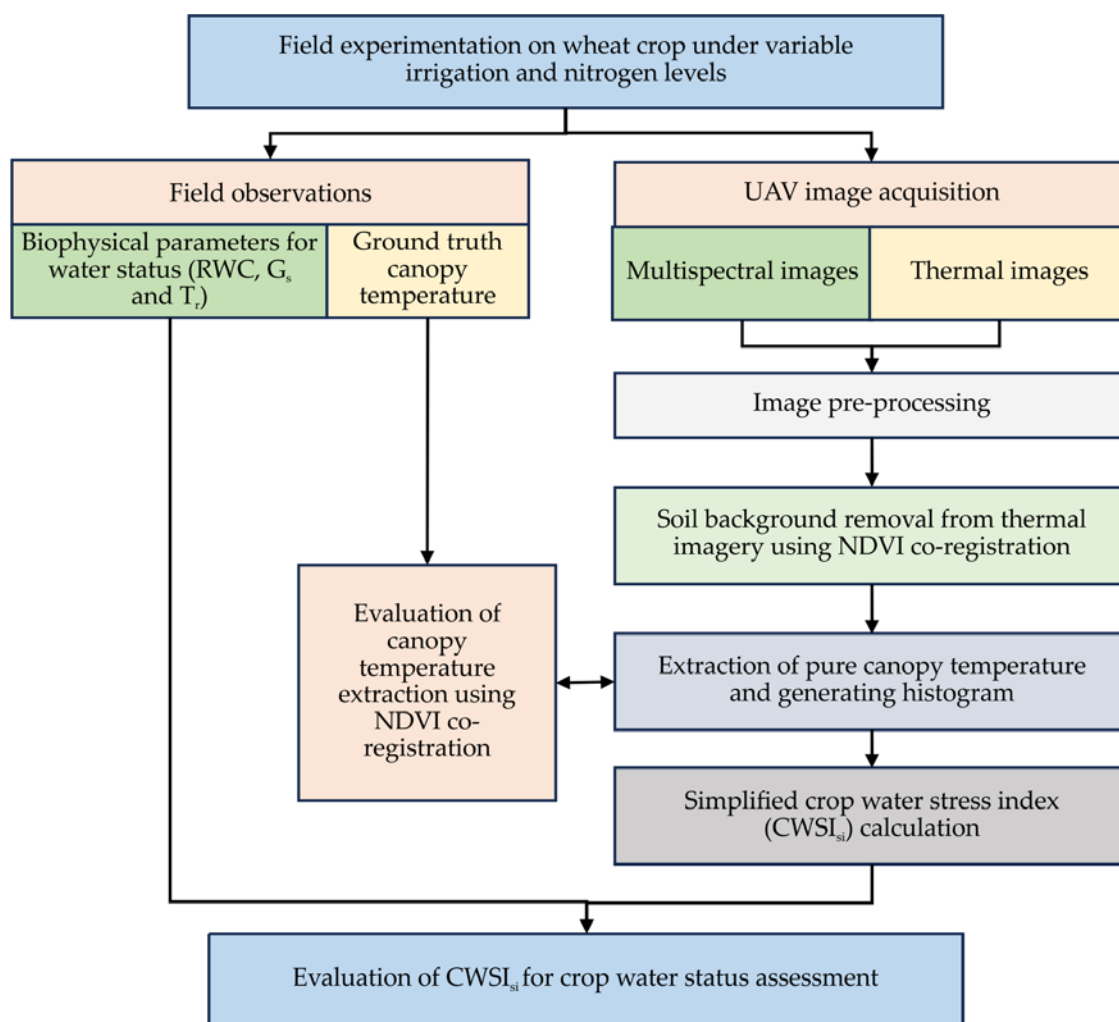


Fig. 4. Workflow of the study

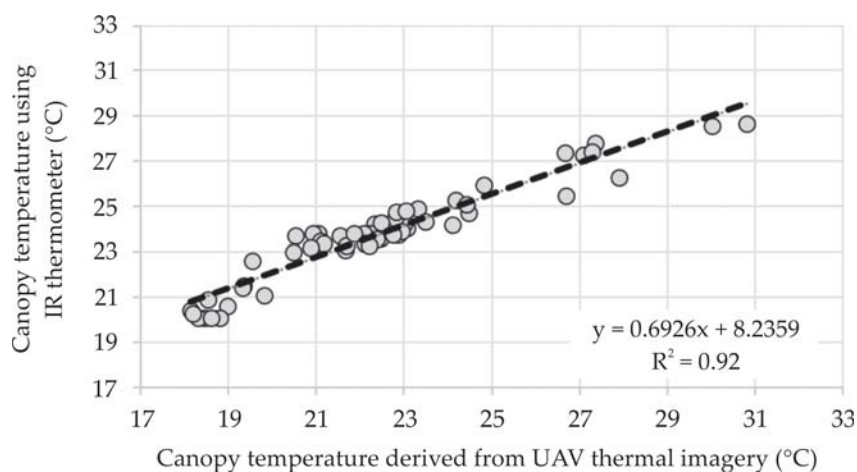


Fig. 5. Relationship between canopy temperatures measured using infrared thermometer (ground truth) and derived from UAV thermal imagery

background effect in handheld IR thermometer measurements than the UAV thermal imageries after soil background removal through NDVI co-registration. Liu *et al.* (2024) found similar linear relationship (with $R^2 = 0.94$) between the wheat canopy temperature from the two sources where soil pixels were removed using a similar NDVI- Otsu method. However, they found higher temperature values from thermal imagery than the ground truth.

Table 2 clearly shows significantly higher canopy temperature in non-irrigated treatments compared to irrigated treatments due to stress induced by water deficiency. However, there was no significant difference of canopy temperature between two times (I2) and five times (I3) irrigation treatments at 95 and 102 DAS as both received 50 mm irrigation at 90 DAS and 11 mm rainfall at 99 DAS. It also showed the significant decrease of canopy temperature with increasing levels of nitrogen dose up to N4 i.e. 120 kg N ha⁻¹ except for non-irrigated treatments (I1) where it increased from N4 to N6 significantly. Studies have shown that nitrogen application can lead to reduced canopy temperature under well-watered conditions (Penuelas *et al.*, 1996; Fois *et al.*, 2009), supporting the positive relationship between nitrogen supply and canopy cooling. Mon *et al.* (2016) also reported cooling in canopy

temperature with nitrogen application in water-limited conditions in durum wheat. The increase in canopy temperature from 120 kg N ha⁻¹ (N4) to 200 kg N ha⁻¹ (N6) under non-irrigated conditions indicates that excessive nitrogen application under water stress can lead to reduced plant water uptake.

Variation of CWSI_{st}, relative leaf water content (RWC), stomatal conductance (Gs) and transpiration rate (Tr)

The Table 3 represents the variation CWSI_{st} and concurrent measurements of RWC, Gs and Tr values averaged over three dates of observation, as influenced by variable irrigation and nitrogen applications. A significant decrease in CWSI_{st} (at $p = 0.05$) was observed from non-irrigated to irrigated treatments. CWSI_{st} also decreased with higher nitrogen doses, significantly up to N4, except in non-irrigated treatments (I1), where it increased from N5 to N6. The highest CWSI_{st} values were found in I1N1 and I1N2, with average values of 0.422 and 0.416, respectively, while the lowest values ranged from 0.168 to 0.184, occurring in I2N6 and I3N4–N6.

RWC exhibited a significant increase with a greater number of irrigations, in the order of I1 < I2 < I3 when averaged across variable nitrogen doses.

Table 2. Influence of different levels of irrigation and nitrogen on wheat canopy temperature

	N1	N2	N3	N4	N5	N6	Avg.
Average Canopy temperature (°C) at 95 DAS							
I1	30.80 ^a	30.02 ^b	27.90 ^c	26.66 ^e	26.69 ^e	27.34 ^d	28.24 ^A
I2	24.47 ^f	23.31 ^h	23.07 ⁱ	22.32 ^{kl}	22.23 ^{klm}	22.07 ^m	22.91 ^B
I3	24.09 ^g	23.49 ^h	22.86 ⁱ	22.47 ^j	22.37 ^{jk}	22.10 ^{lm}	22.90 ^B
Avg.	26.46 ^A	25.61 ^B	24.61 ^C	23.82 ^D	23.77 ^D	23.84 ^D	
Average Canopy temperature (°C) at 102 DAS							
I1	23.02 ^a	22.8 ^b	21.03 ^d	20.52 ^e	20.92 ^d	21.53 ^c	21.64 ^A
I2	19.55 ^g	18.52 ^k	19.34 ^h	18.97 ⁱ	18.44 ^{kl}	18.19 ^m	18.83 ^B
I3	19.31 ^h	19.81 ^f	18.79 ^j	18.29 ^{lm}	18.59 ^k	18.18 ^m	18.83 ^B
Avg.	20.63 ^A	20.37 ^B	19.72 ^C	19.26 ^D	19.32 ^D	19.28 ^D	
Average Canopy temperature (°C) at 109 DAS							
I1	27.09 ^a	27.28 ^a	24.80 ^b	24.18 ^d	22.81 ^f	24.42 ^c	25.10 ^A
I2	22.94 ^{ef}	22.19 ^h	22.75 ^f	21.66 ⁱ	21.69 ⁱ	21.08 ^j	22.05 ^B
I3	23.03 ^e	22.47 ^g	21.86 ⁱ	21.17 ^j	20.87 ^k	20.48 ^l	21.65 ^C
Avg.	24.35 ^A	23.98 ^B	23.14 ^C	22.34 ^D	21.99 ^E	21.79 ^F	

#Values for each DAS followed by the same letters are not significantly different at $P = .05$ as per DMRT. The uppercase and lowercase letters are used for main effects and interaction effects, respectively.

Table 3. Variation of average CWSI_{si}, relative leaf water content (RWC), stomatal conductance (Gs) and transpiration rate (Tr) of wheat under different irrigation and nitrogen levels

Treatments		CWSI _{si}	RWC (%)	Gs (mol H ₂ O m ⁻² s ⁻¹)	Tr (mmol H ₂ O m ⁻² s ⁻¹)
Irrigation					
I1		0.347 ^A	87.41 ^A	0.198 ^A	3.66 ^A
I2		0.210 ^B	91.29 ^B	0.250 ^B	5.01 ^B
I3		0.201 ^C	91.74 ^C	0.306 ^C	5.92 ^C
Nitrogen					
N1		0.304 ^A	88.35 ^A	0.189 ^A	3.71 ^A
N2		0.284 ^B	89.52 ^B	0.209 ^B	4.28 ^B
N3		0.255 ^C	90.13 ^C	0.251 ^C	4.85 ^C
N4		0.229 ^D	90.89 ^D	0.281 ^D	5.34 ^D
N5		0.220 ^D	91.18 ^D	0.288 ^{DE}	5.49 ^D
N6		0.223 ^D	90.80 ^D	0.292 ^E	5.50 ^D
Irrigation × Nitrogen					
I1	N1	0.422 ^a	85.39 ^a	0.153 ^a	2.85 ^a
	N2	0.416 ^a	86.70 ^b	0.170 ^a	3.11 ^a
	N3	0.331 ^b	88.04 ^c	0.197 ^b	3.56 ^b
	N4	0.302 ^c	88.35 ^c	0.223 ^{cde}	4.13 ^{cd}
	N5	0.285 ^c	88.75 ^c	0.228 ^{de}	4.25 ^{cd}
	N6	0.326 ^b	87.23 ^b	0.219 ^{cd}	4.05 ^{cd}
I2	N1	0.247 ^d	89.57 ^d	0.194 ^b	3.91 ^{bc}
	N2	0.215 ^{fg}	90.91 ^e	0.207 ^{bc}	4.40 ^d
	N3	0.227 ^{def}	90.93 ^e	0.242 ^{ef}	4.91 ^e
	N4	0.200 ^{ghi}	91.88 ^{fg}	0.277 ^g	5.42 ^{fg}
	N5	0.192 ^{hi}	92.03 ^{fgh}	0.285 ^g	5.63 ^{fg}
	N6	0.176 ^{ij}	92.40 ^{gh}	0.295 ^{gh}	5.76 ^{gh}
I3	N1	0.243 ^{de}	90.10 ^d	0.220 ^{cd}	4.36 ^d
	N2	0.222 ^{efg}	90.96 ^e	0.249 ^f	5.32 ^{fg}
	N3	0.206 ^{fgh}	91.41 ^{ef}	0.312 ^h	6.06 ^h
	N4	0.184 ^{hij}	92.44 ^{gh}	0.345 ⁱ	6.49 ⁱ
	N5	0.182 ^{ij}	92.76 ^h	0.350 ⁱ	6.61 ⁱ
	N6	0.168 ^j	92.77 ^h	0.363 ⁱ	6.68 ⁱ

#Values for each column followed by the same letters are not significantly different at $P = .05$ as per DMRT. The uppercase and lowercase letters are used for main effects and interaction effects, respectively.

With increased nitrogen, RWC rose significantly upto N4, beyond which there was no further significant difference except in non-irrigated (I1) conditions, where it decreased significantly from N5 to N6 by 1.52 %.

Stomatal conductance (G_s) showed minimum values in I1N1 (average 0.153 mol H₂O m⁻²s⁻¹) and I1N2 (average 0.170 mol H₂O m⁻²s⁻¹), and maximum values in I3N4, I3N5, and I3N6 (averaging 0.345 to

0.363 mol H₂O m⁻²s⁻¹). Average G_s values showed significant differences by irrigation level in order of $I1 < I2 < I3$. When averaged across irrigation levels, G_s increased significantly with nitrogen dose, with all levels showing significant differences except between N5 and N6. Under non-irrigated conditions, a non-significant decrease in G_s was observed between N5 and N6. Similar effect was observed in case of transpiration rate (T_r), as well, where it was

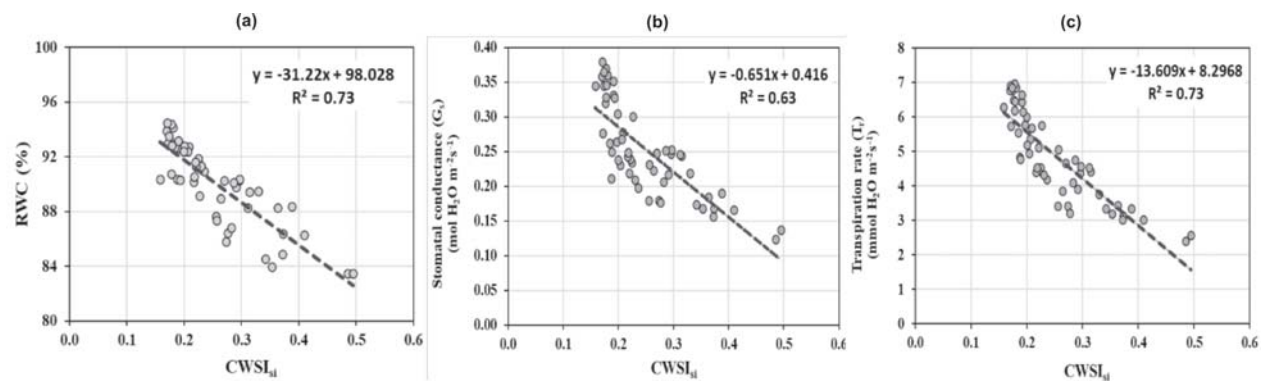


Fig. 6. Relationship between $CWSI_{si}$ and (a) relative leaf water content (RWC), (b) stomatal conductance (G_s), (c) transpiration rate (Tr) of wheat under different irrigation and nitrogen levels

lowest in I1N1 and I1N2, averaging 2.85 and 3.11 $mmol H_2O m^{-2} s^{-1}$, respectively. The highest Tr values were recorded in I3N4, I3N5, and I3N6, averaging between 6.49 and 6.68 $mmol H_2O m^{-2} s^{-1}$. The RWC, G_s and Tr were found to be increasing with increasing nitrogen doses (significantly up to N4) as fertilizers stimulate the growth of transpiring vegetative surface and it may also encourage deeper root development, resulting in better soil moisture extraction (Shimshi and Kafkafi, 1978). However, under non-irrigated conditions (I1), the values reduced from N5 to N6 (RWC decreased significantly but changes in G_s and Tr were not statistically significant). Yang *et al.* (2018) similarly observed that supplemental irrigation and nitrogen boosted stomatal conductance and transpiration rate in winter wheat except at later stage where those decreased with large applications of nitrogen under water deficit treatments. Reduction in these biophysical parameters under water deficit but high nitrogen application (beyond 160 kg N ha^{-1}) can possibly be attributed to higher osmotic concentration of nitrogen in soil solution.

Correlation among $CWSI_{si}$, relative leaf water content (RWC), stomatal conductance (G_s) and transpiration rate (Tr)

The relationship between $CWSI_{si}$ with biophysical parameters of crop water status (RWC, G_s and Tr) are presented in Fig. 6. Results showed negative linear relationships between the $CWSI_{si}$ and biophysical parameters with R^2 of 0.73, 0.63 and 0.73 for relative leaf water content (%), stomatal conductance ($mol H_2O m^{-2} s^{-1}$) and transpiration rate

($mmol H_2O m^{-2} s^{-1}$), respectively. These relationships suggest that those water status parameters can be determined based on the $CWSI_{si}$ approach under various irrigation and nitrogen regimes, thus enabling determination of water status of the crop through the $CWSI_{si}$ values. Pearson's correlation coefficient (r) was calculated among $CWSI_{si}$, RWC, G_s and Tr . Average $CWSI_{si}$ is strongly negatively correlated with crop water status ($r = -0.793$ for G_s , -0.855 for RWC, and -0.857 for Tr). It signifies that increased water stress reduces relative water content, stomatal conductance and transpiration rate as the plants tends to conserve water by limiting stomatal exchanges. These findings are consistent with Bian *et al.* (2019), who reported similar correlations with stomatal conductance ($R^2 = 0.66$) and transpiration rate ($R^2 = 0.59$) in cotton under variable irrigation treatments. Notably, their study found $CWSI_{si}$ to outperform empirical CWSI, statistical CWSI, and multispectral indices (NDVI, TCARI, OSAVI, TCARI/OSAVI) in terms of correlation strength. The findings are also corroborated by the studies of Ramos-Fernández *et al.* (2024) and Wang *et al.* (2024), confirming the reliability of the $CWSI_{si}$.

Conclusion

This study highlights the potential of application of UAV thermal imagery for water status assessment under diverse irrigation and nitrogen management in wheat crop. The strong correlation between $CWSI_{si}$ and biophysical water status parameters such as RWC, transpiration rate and stomatal conductance suggests that it can serve as a reliable, real-time tool

to optimize irrigation and nitrogen management by timely detection of water stress. However, these correlations and empirical relationships are prone to be affected by crop types, growth stages, soil types, pest and disease infestations etc. The future research may be conducted on different other cereals, commercial and high value field crops throughout their growing period. Application of multi-sensor approaches such as utilizing thermal imaging with hyperspectral data acquisition may address those limitations and can help to develop a scalable model for wide adaptation of UAV remote sensing technology by farmers and other stakeholders for sustainable water and nutrient management.

Acknowledgements

The research was conducted under the ICAR-Network Program on Precision Agriculture, operating within the Division of Agricultural Physics at Indian Agricultural Research Institute (IARI), New Delhi with financial support from ICAR, which is gratefully acknowledged. The first author also acknowledges the financial support provided by ICAR, New Delhi as scholarship during his MSc studies.

References

- Arndt, S.K., Irawan, A. and Sanders, G.J. 2015. Apoplastic water fraction and rehydration techniques introduce significant errors in measurements of relative water content and osmotic potential in plant leaves. *Physiologia Plantarum* **155**(3): 355–368. <https://doi.org/10.1111/ppl.12380>
- Balota, M., Payne, W.A., Evett, S.R. and Lazar, M.D. 2007. Canopy temperature depression sampling to assess grain yield and genotypic differentiation in winter wheat. *Crop Science* **47**(4): 1518–1529. <https://doi.org/10.2135/cropsci2006.06.0383>
- Bashir, M.A., Hata, T., Tanakamaru, H., Abdelhadi, A.W. and Tada, A. 2008. Satellite-based energy balance model to estimate seasonal evapo-transpiration for irrigated sorghum: A case study from the Gezira scheme, Sudan. *Hydrology and Earth System Sciences* **12**(4): 1129–1139. <https://doi.org/10.5194/hess-12-1129-2008>
- Bian, J., Zhang, Z., Chen, J., Chen, H., Cui, C., Li, X. and Fu, Q. 2019. Simplified evaluation of cotton water stress using high-resolution unmanned aerial vehicle thermal imagery. *Remote Sensing* **11**(3): 267. <https://doi.org/10.3390/rs11030267>
- Evans, J.R. and Santiago, L.S. 2014. Prometheus Wiki Gold Leaf Protocol: gas exchange using LI-COR 6400. *Functional Plant Biology* **41**(3): 223–226. <http://dx.doi.org/10.1071/FP10900>
- Fois, S., Motzo, R. and Giunta, F. 2009. The effect of nitrogenous fertilizer application on leaf traits in durum wheat in relation to grain yield and development. *Field Crops Research* **110**(1): 69–75. <https://doi.org/10.1016/j.fcr.2008.07.004>
- Gago, J., Douthe, C., Florez-Sarasa, I., Escalona, J.M., Galmes, J., Fernie, A.R., Flexas, J. and Medrano, H. 2014. Opportunities for improving leaf water use efficiency under climate change conditions. *Plant Science* **226**: 108–119. <https://doi.org/10.1016/j.plantsci.2014.04.007>
- Idso, S.B., Jackson, R.D. and Reginato, R.J. 1977. Remote sensing of crop yields: Canopy temperature and albedo measurements have been quantitatively correlated with final harvests of wheat. *Science* **196**(4285): 19–25. <https://doi.org/10.1126/science.196.4285.19>
- Idso, S.B., Jackson, R.D., Pinter, P.J., Reginato, R.J. and Hatfield, J.L. 1981. Normalizing the Stress Degree Day Parameter for Environmental Variability. *Agricultural Meteorology* **24**: 45–55. [http://dx.doi.org/10.1016/0002-1571\(81\)90032-7](http://dx.doi.org/10.1016/0002-1571(81)90032-7)
- Jackson, R.D., Reginato, R.J. and Idso, S.B. 1977. Wheat canopy temperature: A practical tool for evaluating water requirements. *Water Resources Research* **13**(3): 651–656. <https://doi.org/10.1029/WR013i003p00651>
- Liu, H., Song, W., Ly, J., Gui, R., Shi, Y., Lu, Y., Li, M., Chen, L. and Chen, X. 2024. Precise drought threshold monitoring in winter wheat using the unmanned aerial vehicle thermal method. *Remote Sensing* **16**(4): 710. <https://doi.org/10.3390/rs16040710>
- Ministry of Agriculture and Farmers Welfare, Government of India. 2017. Agricultural statistics at a glance 2016. <https://eands.da.gov.in/PDF/Glance-2016.pdf> (last access: 5 October, 2024).
- Mon, J., Bronson, K.F., Hunsaker, D.J., Thorp, K.R., White, J.W. and French, A.N. 2016. Interactive effects of nitrogen fertilization and irrigation on grain yield, canopy temperature, and nitrogen

- use efficiency in overhead sprinkler-irrigated durum wheat. *Field Crops Research* **191**: 54–65. <https://doi.org/10.1016/j.fcr.2016.02.011>
- Nielsen, D.C. and Halvorson, A.D. 1991. Nitrogen fertility influence on water stress and yield of winter wheat. *Agronomy Journal* **83**(6): 1065-1070. <http://dx.doi.org/10.2134/agronj1991.00021962008300060025x>
- Penuelas, J., Filella, I., Serrano, L. and Save, R. 1996. Cell wall elasticity and water index (R970 nm/R900 nm) in wheat under different nitrogen availabilities. *International Journal of Remote Sensing* **17**(2): 373–382. <https://doi.org/10.1080/01431169608949012>
- Ramos-Fernández, L., Gonzales-Quiquia, M., Huanqueño-Murillo, J., Tito-Quispe, D., Heros-Aguilar, E., Flores del Pino, L. and Torres-Rua, A. 2024. Water stress index and stomatal conductance under different irrigation regimes with thermal sensors in rice fields on the northern coast of Peru. *Remote Sensing* **16**(5): 796. <https://doi.org/10.3390/rs16050796>
- Sadras, V.O. 2004. Yield and water use efficiency of water- and nitrogen-stressed wheat crops increase with degree of co-limitation. *European Journal of Agronomy* **21**(4): 455–464. <https://doi.org/10.1016/j.eja.2004.07.007>
- Shimshi, D. and Kafkafi, U. 1978. The effect of supplemental irrigation and nitrogen fertilization on wheat (*Triticum aestivum* L.). *Irrigation Science* **1**(1): 27–38. <https://doi.org/10.1007/BF00269005>
- Wang, C., Zhu, K., Bai, Y., Li, C., Li, M. and Sun, Y. 2024. Response of stomatal conductance to plant water stress in buffalograss seed production: Observation with UAV thermal infrared imagery. *Agricultural Water Management* **292**: 108661. <https://doi.org/10.1016/j.agwat.2023.108661>
- Yang, D.Q., Dong, W.H., Luo, Y.L., Song, W.T., Cai, T., Li, Y. and Wang, J.L. 2018. Effects of nitrogen application and supplemental irrigation on canopy temperature and photosynthetic characteristics in winter wheat. *The Journal of Agricultural Science* **156**(1): 13–23. <https://doi.org/10.1017/S0021859617000946>
- Zhou, Z., Majeed, Y., Naranjo, G.D. and Gambacorta, E.M.T. 2021. Assessment for crop water stress with infrared thermal imagery in precision agriculture: A review and future prospects for deep learning applications. *Computers and Electronics in Agriculture* **182**: 106019. <https://doi.org/10.1016/j.compag.2021.106019>

Received: 17 July 2024; Accepted: 3 October 2024